Revista de Chimie
https://revistadechimie.ro
https://doi.org/10.37358/Rev.Chim.1949

Synthesis of Poly (Styrene Sulfonate) Coated Gd^{3+} Poly (Lactide-Co-Glycolic Acid) Perfluoro Bromide Nanoparticles for Stem Cell Monitoring Using Magnetic Resonance Imaging

HIEU VU-QUANG[1,2*], THANH-QUANG NGUYEN[3], MADS SLOTH VINDING[4]
[1] NTT - Hitech Institute, Nguyen Tat Thanh University, 298-300 Nguyen Tat Thanh, Ho Chi Minh city, Vietnam
[2] Interdisciplinary Nanoscience Center (iNANO), Aarhus University, Gustav Wieds Vej 14, 8000 Aarhus C, Denmark
[3] Department of Cooperation and Research, Van Lang University, 45 Nguyen Khac Nhu, Ho Chi Minh city, Vietnam
[4] Center of Functionally Integrative Neuroscience (CFIN), Department of Clinical Medicine, Aarhus University Hospital, Palle Juul-Jensen Boulevard 99, 8200 Aarhus N, Denmark

Abstract. *Magnetic resonance imaging (MRI) is one of best imaging technologies to monitor transplanted stem cells, because of its high anatomical resolution and safety. In this study, we aim to synthesize Poly (styrene sulphonate) coated Gd^{3+} - Poly (lactide co glycolic acid) Perfluorooctyl Bromide nanoparticles (PSS-coated Gd^{3+}@NPs) for stem cell labeling using both ^{1}H and ^{19}F MRI. At a weight ratio 20 of PLGA/ Gd^{3+}, NPs have a spherical shape with the hydrodynamic size at 180 nm with zeta potential at -53 mV. In vitro, we obtain the intended T1 relaxation acceleration of water on ^{1}H MRI. The NPs have low toxicity to the human mesenchymal stem cells (hMSC) up to 1 mg/ml. They could internalize into the stem cells via caveolae-mediated endocytosis efficiently, confirmed by flow cytometry analysis, and gives a good contrast in both channels ^{1}H and ^{18}F MRI scans. In conclusion, our NPs have shown a great potential as a dual-contrast agent in MRI for stem cell monitoring.*

Keywords*: MRI contrast agent, gadolinium, perfluorooccctyl bromide, stem cell monitoring*

1. Introduction

Rising incidence of degenerative diseases such as osteoarthritis and neurological disorders has pressed the demand for regenerative therapies in countries with aging population. The treatment of these diseases often consists of several approaches. Among them, stem cell therapy, which involves transplantation of stem cells to the patient, is one of the potential methods in regenerative medicine that could assist the treatment of such diseases. Transplanted stem cells will alter into targeted cells in order to cure and replace the damaged cells. However, for safety and prognostic reasons, the transplanted stem cells need to be tracked and monitored *in vivo*.

Magnetic resonance imaging (MRI) is a versatile imaging technique that provides a tool for monitoring the stem cells after transplantation. Prior to transplantation, stem cells are labeled with contrast agents such as super paramagnetic iron oxides nanoparticles (SPION), Gadolinium containing compounds, or fluorinated nanoparticles in order to be detected using MRI [1-4]. Among these three contrast agents, SPION is mostly used for its high sensitivity in ^{1}H MRI and its ability to create a negative contrast (darkness) in the images. However, the signal of the SPION labeled stem cells can be confused with other tissues having inherently low T2 relaxation times, such as hemorrhage, bone, and air. Moreover, the magnetic susceptible effects of SPION labeled cells can also result in a blooming artifact that surpasses the size of an individual cell, thereby obscuring surrounding anatomy [5-7]. Alternatively, the use of Gadolinium-chelates, which are commonly used intravenous contrast agents to create positive contrast (brightness) in ^{1}H T1 weighted MRI, poses some challenges for medical applications due to their low sensitivity, weak uptake efficiency, and the high toxicity of Gd^{3+} chelates [4]. Fluorinated compounds, usually called tracers rather than contrast agents, provide high nuclear magnetic sensitivity [8-10] without exerting interference with the intrinsic signal sources.

**email: vqhieu@ntt.edu.vn*

Since the amount of fluorine in biological tissue is negligible, ^{19}F MRI signal of labeled cells appears as hot spots with no or only minute background signal in the ^{19}F MR image. Aside from providing accurate and unambiguous detection of labeled cells, the fluorine signal intensity is directly proportional to its concentration, which allows accurate quantification [10-12]. However, currently available ^{19}F probes have limited sensitivity, calling for the designing of new MRI probes that preferably result in improved MRI signal in both ^{1}H and ^{19}F MRI channels.

Based on our previous studies, we found that coating poly(styrene sodium sulphonate) onto poly(lactide -co-glycolic acid) perfluorooctyl bromide nanoparticles (PSS-coated NPs) would be used to label human mesenchymal stem cells (hMSC) for tracking using ^{19}F MRI [13,14]. The hMSC cells, with PSS-coated NPs labels, can be tracked for up to two months. However, the positional information of the stem cell is missing, which challenges anatomical referencing. This again raises the need for fabrication of new contrast agent that provides the specificity and anatomical information necessary for stem cell monitoring. Herein, we aimed to synthesize a nanoparticle that could be both a T1 and fluorinated MRI contrast agent, abbreviated as PSS-coated Gd^{3+}@PLGA PFOB NPs. Then we investigated the relaxation properties of the proposed NPs, which can be used to tailor future scan protocols and adopt the dual contrast mechanisms.

2. Materials and methods

All of the materials were purchased from Sigma Aldrich, St Louis, MO, USA, or otherwise noted.

2.1 Synthesis of Gd^{3+}@PFOB NPs

PSS-coated NPs were formulated by single emulsion evaporation as described before with some modifications [10,15]. In brief, 100 mg of PLGA and 60 µL of PFOB were dissolved in 4 mL of organic phase dichloromethane (DCM). The mixture was emulsified in 20 mL of 1.5% sodium cholate by vortexing and sonicating each for 1 min in an ice bath. The DCM was allowed to evaporate over 6 h with magnetic stirring at 300 rpm. PSS (70 kDa molecular weight) was added to the NPs to yield a final concentration of 1%, followed by incubation for 5 days. The NPs were collected by centrifugation at 2000 rpm for 30 min. The NP were re-suspended in distilled water. The mass of the NPs in water was weighed by freeze-drying. Henceforth, these NPs will be termed PSS-coated NPs and stand as our controls.

For producing PSS-coated Gd^{3+}@NPs, Gd^{3+} DTPA-bis(stearyamide) (DTPA-BSA-Gd^{3+}) (Advanti Polar, USA) was first dissolved in methanol at a concentration of 25 mg/mL. Then, the mixture was added to the organic phase at various weight ratios (with respect to PLGA) from 1/10 to 1/30.

For synthesizing fluorescent NPs to be used in the flow cytometry analysis (FACS), 10 µL of Coumarin 6 in DCM (1 mg/mL) was added to the organic solvent before emulsification.

2.2 Synthesis of microparticles for confocal laser scanning microscope (CLSM) observation

All of the materials with Coumarin 6 in organic phase and water phase were prepared as described above. However, the emulsification process was done using an UltraTurax (IKA, Germany) at 2000 rpm for 2 min in an ice bath. The organic solvent was allowed to evaporate. The samples were then taken and dropped on glass slides for observing the morphology of microparticles.

2.3 Encapsulation efficiency

The NPs (50 µL) after purification were freeze dried, weighed and re-dissolved in $CDCl_3$. The PFOB concentration in the NPs was measured using 400 MHz nuclear magnetic resonance (NMR) spectrometer (Bruker Biospin, Ettlingen, Germany) with Perfluoro-crown-ether as reference concentration.

2.4 Measurement of hydrodynamic size

The hydrodynamic size, polydispersity index (PDI) and zeta potential were measured in deionized water using a Zetasizer Nano ZS from Malvern Instruments Ltd., Worcestershire, UK. The measurements were performed four times at 25°C with a scattering angle of 173°.

2.5 Tranmission electron microscopy

The morphology of the NPs was determined using negative-stain transmission electron microscopy (TEM). A 10 μL aliquot of NPs was loaded onto a carbon film-coated 200 mesh copper grid (Ted Pella Inc., Redding, CA, USA). After 1 min, loaded NPs were stained with 10 μL of uranyl acetate for an additional 30 s. The TEM images were acquired using a TE microscope (Technai G2 Spirit, Oregon, USA) at 120 kV.

2.6 Cytotoxicity assay

hMSC-TERT cells were seeded in 96-well plates (10,000 cells per well) and incubated in growth media overnight. Cells were incubated with PSS-coated NPs, PSS-coated Gd^{3+}@NPs, weight ratio 1/10, 1/20, and 1/30 at concentration 1 mg/mL for 1 day. The cell viability was then measured by an MTT (3-(4,5-Dimethylthiazol-2-yl)- 2,5 diphenyltetrazolium bromide) assay according to the manufacturer's protocol (Promerga, Madison, Wisconsin, USA).

2.7 Cell uptake pathway - Flow cytometry analysis (FACs)

hMSC-TERT was labelled with Coumarin 6 loaded PSS-coated Gd^{3+}@NPs by incubating the cells in growth media containing NPs at a final concentration of 0.5 mg/mL for 4 h in 12-well plates. The cells were washed thoroughly with PBS, harvested and analyzed with the Gallios Flow cytometer (Beckman Coulter, CA, USA). The PSS polymers were added to the media at a final concentration of 0.5 mg/mL before the treatment for competition assay. The PSS polymer would compete with PSS-coated Gd^{3+}@NPs and PSS-coated NPs for caveolae dependent endocytosis.

2.8 *In vitro* ^{19}F and ^{1}H MRI

The MRI experiments were performed on 16.4 Tesla, vertical bore, micro imaging system with the dual-tuned ^{1}H/ ^{19}F coil (Bruker, Elttingen, Germany).

In this study, all NPs were loaded into glass tubes and sunk in a cup of water then centered in the radio frequency coil for scanning. The Gd^{3+} chelate with concentration 0.1 mg/mL in water was used as reference.

2.8.1 Parametric maps

The ^{1}H scans targeting the water content were: Firstly, a T1 map using the Rapid-Acquisition-with-Relaxation-Enhancement-with-Variable-Repetition-Time (RAREVTR) sequence with repetition times (TR) ranging from 100 ms to 10 s in ten steps. The image matrix was 96 by 96 spanning a field of view (FOV) of 2.5 cm. The number of scans (NS) averaged over was 10, the echo time (TE) was 4 ms, and the slice thickness (TH) was 1 mm; Secondly, a T2 map using the Multi-Slice-Multi-Echo (MSME) sequence with 64 by 64 image, 20 TEs ranging from 4 ms to 200 ms, NS 5, TH 1mm; Thirdly, a B1 map using two combined MSME scans to measure and account for the spatial (in)sensitivity, with flip-angle sets (90^o, 180^o) and (45^o, 90^o) with TE 20 ms, TR 5000 ms, NS 5, image matrix 64 by 64.

The ^{19}F scans: T1 and T2 maps of PFOB were done using RAREVTR sequence, extended to include a 12-length echo train, with TE ranging from 4 ms to 300 ms. The image matrix was 32 by 32. TR ranged from 200 ms to 10 s in ten steps. NS 40 and TH 15 mm.

The T1, T2 and B1 maps were processed using MATLAB 2019b (Mathworks, Natick, MA, USA).

2.8.2 Cell images

These experiments were set in order to label, monitor (visually) and evaluate the effect of PSS-coated Gd^{3+}@NPs on the hMSCs *in vitro* using ^{19}F ^{1}H MRI. First, the hMSCs were seeded at a density of 10^6 cells per T75 flask and collected at day 1 and fixed in 4% HCHO at 4°C before ^{19}F-MRI scanning. The PFOB in $CDCl_3$ (3.85 µmol) was used as reference. ^{1}H MRI were taken using Fast Low Angle Shot (FLASH) sequence with TR 100 ms, TE 4 ms, TH 0.5 mm, NS 10, image matrix 64 by 64 and FOV 2.4 cm. ^{19}F MRI images were made with MSME sequence with 5 s, TE 7.64 ms, TH 20 mm, NS 15, image matrix 32 by 32, and FOV 2.4 cm^2.

3. Results and discussions

In this study, we aimed to synthesize a new MRI contrast agent that could enhance the MRI signal in both ^{1}H and ^{19}F MRI scans in order to monitor stem cells after transplantation. The NPs were designed to have a core-to-shell structure, where the liquid fluorine PFOB was located in the core and the PLGA was the shell of the NPs (Scheme 1). The DTPA-BSA-Gd^{3+} was also introduced to the NPs during the synthesis, where the bis(stearylamide) lipid tails were embedded into the particle shell. In MRI, the appearance of Gd^{3+} reduces the T1 relaxation time, thus enhancing the T1 weighted MRI signal, while PFOB provides a stand-alone ^{19}F MRI signal. The PSS-coated layer on the NPs assists the endocytosis of them into the stem cell therefore allowing us to monitor stem cell after transplantation.

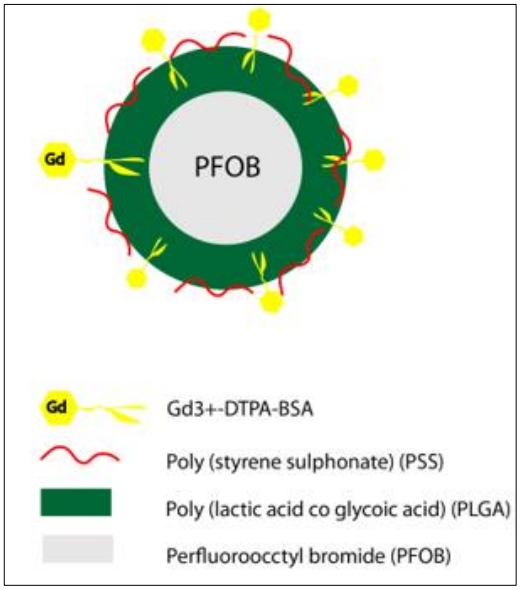

Scheme 1. The design of NPs

3.1 Morphology of particles in the appearance of DTPA-BSA-Gd^{3+}

Morphology and structure of the particles play an important role in the determination of encapsulation efficiency and delivery efficacy. In synthesizing fluorinated NPs, it was reported that the morphology and structure of fluorinated particles were influenced by many factors such as used organic solvents and the ratio of between materials and surfactants. To be specific, it was found that when changing the surfactant from poly vinyl alcohol (PVA) to sodium cholate, the morphology of PLGA PFOB particles were changed from an acorn to a core/shell structure [15,16]. Or, by adding poly(lactic acid) (PLA) to the NPs mixture, the NPs morphology was altered from spherical to ellipsoidal shape [17]. To check the morphology of our particles, when introducing DTPA-BSA-Gd^{3+} to the mixture of polymer, we first observed the size of the obtained NPs. The results displayed in Figure 1 show various morphologies of the obtained NPs. With the presence of DTPA-BSA-Gd^{3+}, the NPs shape changed from core/shell (Figure 1A) to multi-cores/shell (Figure 1B, C). However, at the lower weight ratios, the cores of the particles seemed to be larger than those observed at the higher weight ratio and were similar to the control particles.

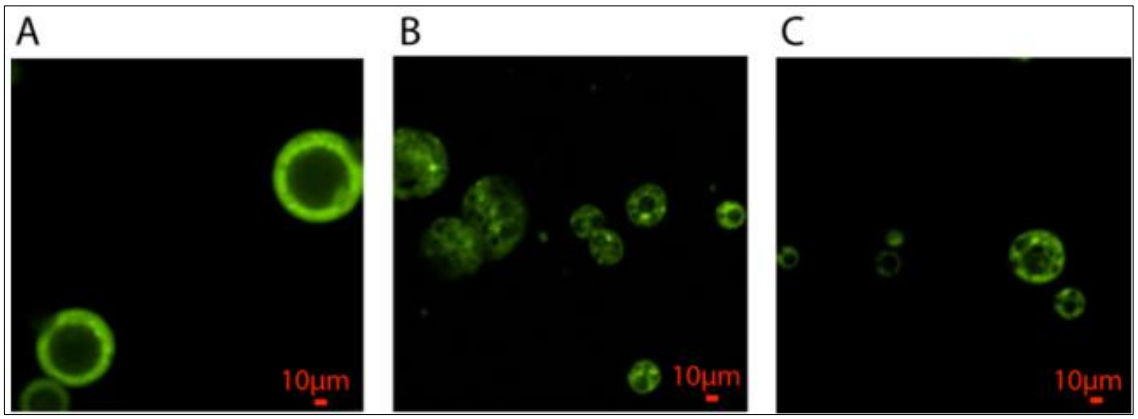

Figure 1. The morphology of microparticles using CLSM. NPs (A), Gd^{3+}@NPs (B) 1/10, (C) 1/20. Scale bar 10 µm

The morphology of particles was further analyzed in the nano regime using TEM. There were some differences between the Gd^{3+}@NPs at weight ratio 1/20 and NPs (Figure 2). All of the NPs had the core/shell structure. However, with weight ratio 1/20, few extra dots appeared on the NPs surface. Since the appearance did not change the entire structure of NPs, these NPs would be evaluated in the subsequent experiments.

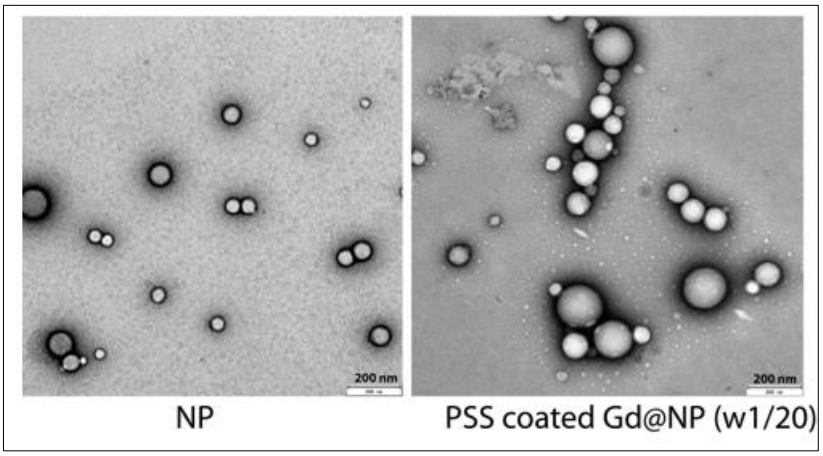

Figure 2. The TEM image of NPs (left) and Gd^{3+} @NPs (right) at weight ratio 1/20. Scale bar 200 nm

3.2 Hydrodynamic size and charge of NPs

After coating NPs with the PSS polymer, the hydrodynamic size and zeta potential were measured. The size and charge of the NPs are presented in Table 1. All NPs had the hydrodynamic size below 200 nm and a high homogeneity poly-dispersity index (PDI < 0.2). The zeta potential of all PSS- and PVA-coated NPs were approximately -50 mV and -10.4 mV, respectively. The negative charge of the PSS-coated NPs could be attributable to the appearance of PSS on the surface of PLGA NPs. This is in line with previous studies on PSS NPs claiming that the hydrophobic chains of PSS bind to the hydrophobic layer of the NPs, while the sulphate group gives the negative charge of NPs [13].

Table 1. Hydro-dynamic size, polydispersity index and zeta potential of various NPs

	Size (nm)	Polydispersity index (PDI)	Zeta Potential (mV)
PVA coated NP	183	0.171	-10.4
PSS coated NP	137	0.156	-50.2
PSS-coated Gd^{3+} @NPs (1/10)	165	0.194	-52.5
PSS-coated Gd^{3+} @NPs (1/20)	188	0.179	-52.9
PSS-coated Gd^{3+} @NPs (1/30)	190	0.175	-50.9

3.3 *In vitro* ^{19}F and ^{1}H MRI

3.3.1 T1

Gd^{3+} is a well-known T1 contrast agent capable of causing faster T1 relaxation in proximity to excited molecules. In this experiment, we evaluated the effect of Gd^{3+} to the MRI signal, especially to T1 relaxation of water (^{1}H) and PFOB (^{19}F).

As shown in the ^{19}F T1 map (Figure 3A), the T1 relaxation time of PFOB in all NPs is approximately 1 second.

For the ^{1}H T1 map (Figure 3B), the T1 relaxation associated with the PSS- and PVA-coated NPs is estimated to range from 2 to 3 s, and slightly lower than that of the T1 of the water in the cup. However, in the with the presence Gd^{3+} at weight ratios 1/10, 1/20, and 1/30, the T1 relaxation time of water were reduced to 1.3 s, 1.8 s and 1.9 s, respectively. The T1 of PSS-coated Gd^{3+}@NPs (weight ratio 1/10) is shorter than those obtained at weight ratios 1/20 and 1/30, which could due to the density of Gd^{3+} on the particles shell. The weight ratio 1/10 presented more Gd^{3+} during the synthesis and thus the T1 of water was shorter.

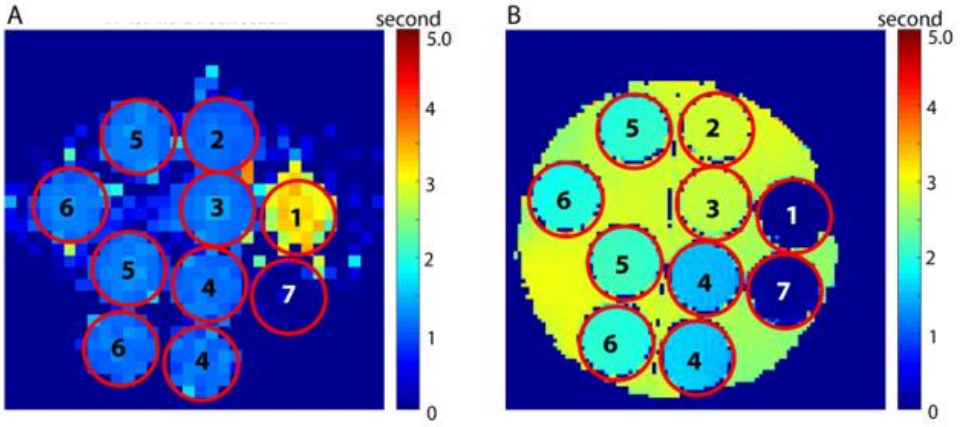

Figure 3. T1 map of NPs on ^{19}F MRI (A) and ^{1}H MRI (B). (1) Reference PFOB in $CDCl_3$ tube, (2) PVA-coated NPs, (3) PSS-coated NPs, (4) PSS-coated Gd^{3+}@NP 1/10, (5) PSS-coated Gd^{3+}@NPs 1/20 and (6) PSS-coated Gd^{3+}@NPs 1/30

3.3.2 T2

Gd^{3+} is a paramagnetic material which also has some mild effects on T2. The Gd^{3+} distorts the surrounding magnetic field and causes a shorter T2. In the ^{19}F MRI (Figure 4A), the T2 of PFOB in the NPs was approximately 0.6 s, however, this value was reduced considerably with the presence of Gd^{3+}. While the ^{1}H T2 (Figure 4B) in the PSS- and PVA-coated NPs was about 0.3 s, the Gd^{3+} NPs had T2 values of around 0.2 s.

The quality our T1 and T2 maps were intended to show trends in different relaxivities. It is possible to increase the accuracy further. The magnetic field strength, in this case 16.4 T, does also affect the relaxation parameters, and the quality in our maps is also reflected by the allocated scans time given.

Our measured relaxation trends are sufficient for the aim that this paper set out for. Furthermore, the image contrasts are shown in the next section.

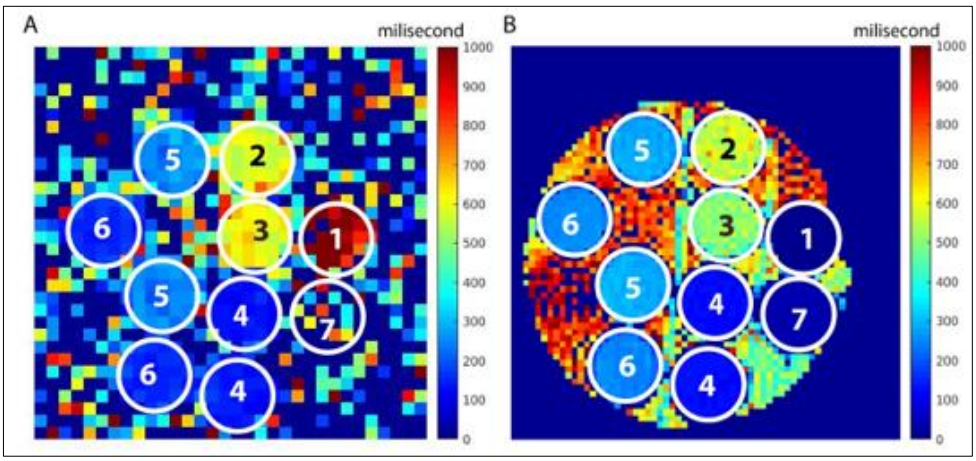

Figure 4. T2 map of NPs in ^{19}F MRI (A) and ^{1}H MRI (B). (1) Reference PFOB in $CDCl_3$ tube, (2) PVA-coated NPs, (3) PSS-coated NPs, (4) PSS-coated Gd^{3+}@NPs 1/10, (5) PSS-coated Gd^{3+}@NPs 1/20 and (6) PSS-coated Gd^{3+}@NPs 1/30

3.4 Cell viability

The effect of NPs to the cell was evaluated using MTT assay. It was showed that the effect of NPs on the cell viability was negligible (Figure 5). All cell viabilities at various concentrations and DPTA-Gd^{3+}-BSA ratios were above 90% after one-day incubation. This suggests that the NPs were safe for cell labeling at the concentration of up to 1 mg/mL and the ratio of Gd^{3+} at weight ratio 1/20 in the NPs.

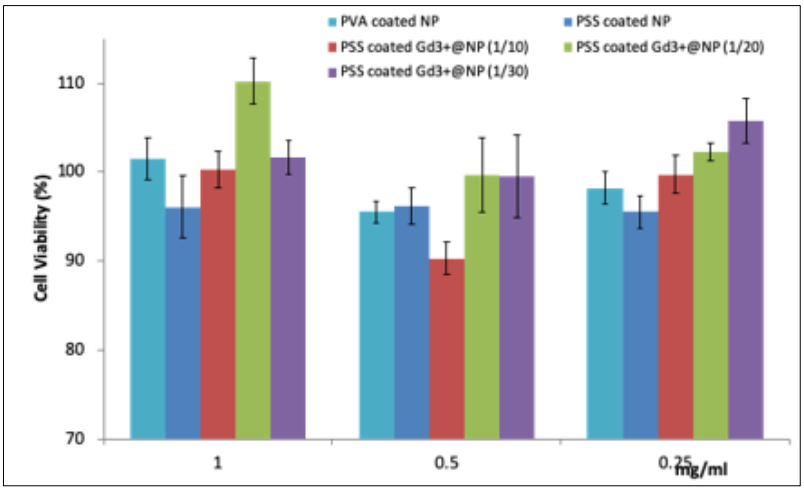

Figure 5. Cell viability of hMSC with various NPs

3.5 Cell uptake pathway

Previous studies have determined that the PSS NPs could internalize into cell *via* caveolae endocytosis pathway [10,13]. Thus, in this experiment, we evaluated the endocytosis of our newly synthesized NPs using FACs. Two comparisons were done to assess accumulation of PSS NPs into hMSC. Firstly, the PSS-coated and PSS-coated Gd^{3+}@NPs at weight ratios 1/10, 1/20 and 1/30 were compared to PVA-coated NPs. As shown in Figure 6, the mean fluorescent intensity of PSS-coated NPs and PSS-coated Gd^{3+}@NPs were significantly higher than that of the PVA-coated NPs. The PSS-coated Gd^{3+}@NPs at all weight ratios showed fluorescent intensities identical to that of PSS-coated NPs. This supports successful internalization of PSS-coated NPs into the cells and indicates that the appearance of Gd^{3+}-DTPA-BSA did not influence the uptake. In the second comparison, the internalization of PSS-

coated Gd^{3+}@NPs *via* the caveolae-endocystosis pathway was realized by adding free PSS into the cell culture media, thus co-incubating with the hMSC. The free PSS polymer would serve as the competitor with the PSS-coated Gd^{3+}@NPs. In the presence of free PSS polymer, the mean fluorescent intensity exhibited by PSS-coated Gd^{3+}@NPs was reduced and was equal to that of PVA-coated NPs. This could be explained by the higher concentration and lower weight of free PSS in the incubated media in comparison with those of PSS on the NPs, accelerating their binding onto the caveolae structure and thus causing their internalization into the hMSC to occur more quickly than into PSS-coated Gd^{3+}@NPs. This resulted in reduced number of PSS-coated NPs entering the hMSC and decreased fluorescent intensity. In summary, the PSS-coated Gd^{3+}@NPs internalize into the cell via the caveolae pathway.

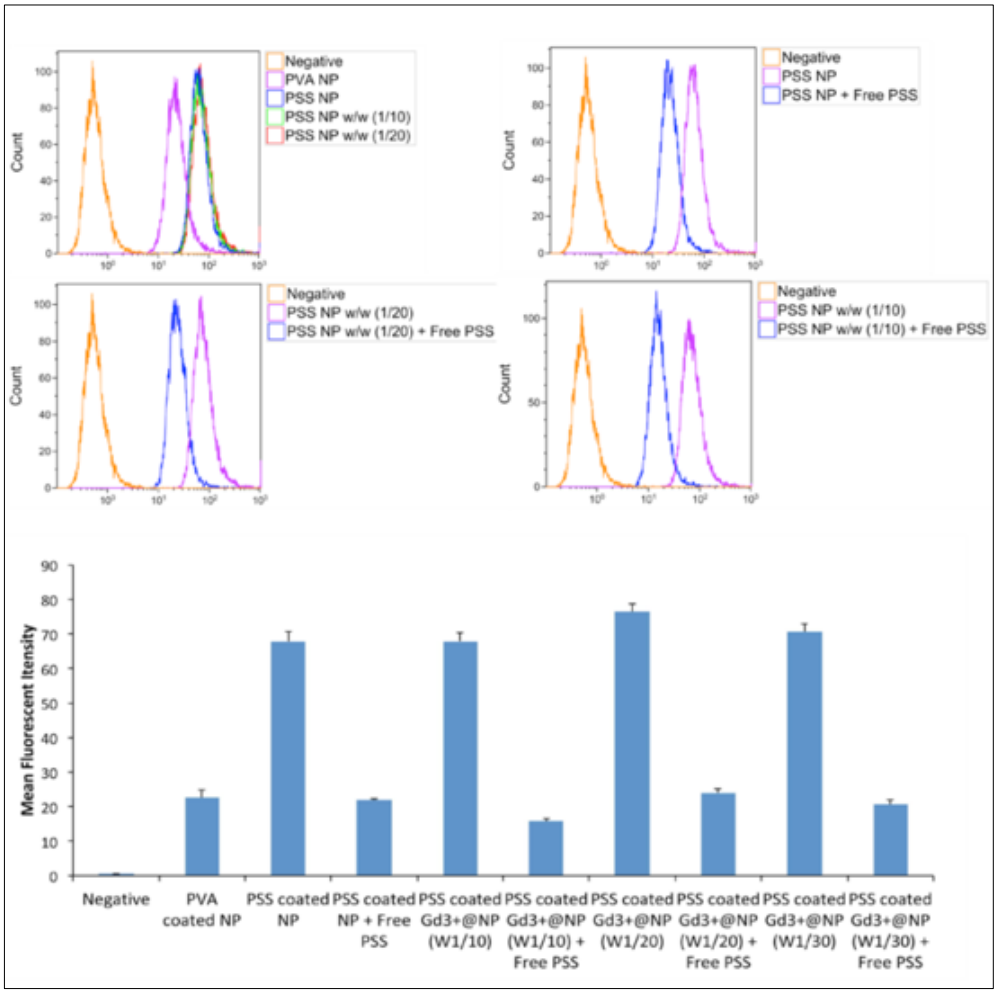

Figure 6. Flow cytometry analysis of PSS-coated Gd^{3+}@NPs at 1/10, 1/20 and 1/30. Control particles are PSS-coated NPs and PVA-coated NPs. The free PSS is a competitor for proving the internalization of PSS particle via caveolae endocytosis pathway. Number of cell count 10.000, number of replication 4

3.6 Cell images

Doubling imaging contrast mechanisms are advantageous for monitoring of cells after transplantation. As shown in the Figure 7, our proposed NPs would give dual MRI hMSC contrasts. Firstly, the added Gd^{3+} accelerates T1 relaxation, which can be exploited in T1 weighted scans, and the cells that embedded the PSS-coated Gd^{3+}@NPs showed a brighter ^{1}H MRI signal compared to those of the controls. Secondly, the PFOB presence in the cells gave a unique ^{19}F MRI contrast. Both PSS-coated Gd^{3+}@NPs and PSS-coated NP yielded the specific ^{19}F MRI signals the cell pellets, demonstrating that the addition of Gd^{3+}-DPTA-BSA does not hamper the ^{19}F benefit and thus the PSS-coated Gd^{3+}@NPs

possess a dual contrast mechanism to be exploited in both ^{1}H and ^{19}F MRI.

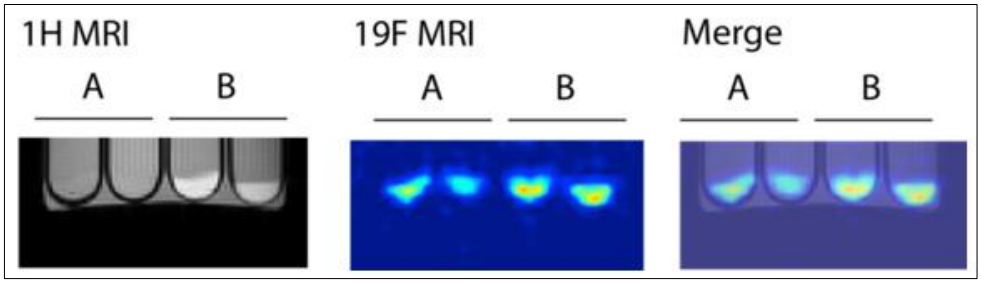

Figure 7. MRI imaging of cell that labeled with PSS-coated NPs and PSS-coated Gd^{3+}@NPs (1/20)

4. Conclusions

In the study, we have successfully synthesized PSS-coated Gd^{3+}@NPs for labelling the hMSC cell. The particle size was smaller than 200 nm with high homogeneity, and had low negative charge, suggesting the potential for cell labeling and monitoring. The PSS-coated Gd^{3+}@NPs may possess multiple cores and different PFOB encapsulation efficiencies depending on the Gd dose, which may be advantageous in developments and designs of other tracers and drug carriers. In the ^{1}H MRI, the Gd^{3+} showed both T1 and T2 effects, whereas in the ^{19}F MRI, perturbation of Gd^{3+} was observed only in the T2. In the *in vitro* MRI, we observed the expected dual contrast mechanisms, i.e., in both ^{19}F and ^{1}H scans of hMSC cell labeled with PSS-coated Gd^{3+}@NPs. Our data suggest that the NPs internalize into the cell via the caveolae endocytosis pathway.

Acknowledgments: Thanks to Professor Kjems' laboratory and Professor Niels Christian Nielsen 's laboratory, Aarhus University for supporting working space and materials. We also thanks to the partly funding (2019/01/19) from Nguyen Tat Thanh university for this research.

References

1.KNIGHT, J.C.; EDWARDS, P.G.; PAISEY, S.J., Fluorinated contrast agents for magnetic resonance imaging; a review of recent developments, *RSC Advances*, ***1***(8), 2011, 1415-1425
2.MANAGH, A.J.; EDWARDS, S.L.; BUSHELL, A.; WOOD, K.J.; GEISSLER, E.K.; HUTCHINSON, J.A.; HUTCHINSON, R.W.; REID, H.J.; SHARP, B.L., Single Cell Tracking of Gadolinium Labeled CD4+ T Cells by Laser Ablation Inductively Coupled Plasma Mass Spectrometry, *Analytical Chemistry*, ***85***(22), 2013, 10627-10634
3.GENG, K.; YANG, Z.X.; HUANG, D.; YI, M.; JIA, Y.; YAN, G.; CHENG, X.; WU, R., Tracking of mesenchymal stem cells labeled with gadolinium diethylenetriamine pentaacetic acid by 7T magnetic resonance imaging in a model of cerebral ischemia, *Mol Med Rep*, ***11***(2), 2015, 954-960
4.ROGOSNITZKY, M.; BRANCH, S., Gadolinium-based contrast agent toxicity: a review of known and proposed mechanisms, *Biometals*, ***29***(3), 2016, 365-376
5.BUDDE, M.D.; FRANK, J.A., Magnetic Tagging of Therapeutic Cells for MRI, *Journal of Nuclear Medicine*, ***50***(2), 2009, 171-174
6.VU-QUANG, H.; MUTHIAH, M.; LEE, H.J.; KIM, Y.-K.; RHEE, J.H.; LEE, J.-H.; CHO, C.-S.; CHOI, Y.-J.; JEONG, Y.Y.; PARK, I.-K., Immune cell-specific delivery of beta-glucan-coated iron oxide nanoparticles for diagnosing liver metastasis by MR imaging, *Carbohydrate Polymers*, ***87***(2), 2012, 1159-1168
7.YANG, C.; VU-QUANG, H.; HUSUM, D.M.U.; TINGSKOV, S.J.; VINDING, M.S.; NIELSEN, T.; SONG, P.; NIELSEN, N.C.; NØRREGAARD, R.; KJEMS, J., Theranostic poly(lactic-co-glycolic acid) nanoparticle for magnetic resonance/infrared fluorescence bimodal imaging and efficient siRNA delivery to macrophages and its evaluation in a kidney injury model, *Nanomedicine: Nanotechnology, Biology and Medicine*, ***13***(8), 2017, 2451-2462

8.DIOU, O.; FATTAL, E.; DELPLACE, V.; MACKIEWICZ, N.; NICOLAS, J.; MERIAUX, S.; VALETTE, J.; ROBIC, C.; TSAPIS, N., RGD decoration of PEGylated polyester nanocapsules of perfluorooctyl bromide for tumor imaging: influence of pre or post-functionalization on capsule morphology, *Eur. J. Pharm. Biopharm.*, ***87***(1), 2014, 170-177
9.VU-QUANG, H.; VINDING, M.S.; NIELSEN, T.; ULLISCH, M.G.; NIELSEN, N.C.; KJEMS, J., Theranostic tumor targeted nanoparticles combining drug delivery with dual near infrared and (19)F magnetic resonance imaging modalities, *Nanomedicine*, ***12***(7), 2016, 1873-1884
10.QUANG, H.V.; CHANG, C.C.; SONG, P.; HAUGE, E.M.; KJEMS, J., Caveolae-mediated mesenchymal stem cell labelling by PSS-coated PLGA PFOB nano-contrast agent for MRI, *Theranostics*, ***8***(10), 2018, 2657-2671
11.FOX, M.S.; GAUDET, J.M.; FOSTER, P.J., Fluorine-19 MRI Contrast Agents for Cell Tracking and Lung Imaging, *Magn Reson Insights*, ***8***(Suppl 1), 2016, 53-67
12.FINK, C.; GAUDET, J.M.; FOX, M.S.; BHATT, S.; VISWANATHAN, S.; SMITH, M.; CHIN, J.; FOSTER, P.J.; DEKABAN, G.A., 19F-perfluorocarbon-labeled human peripheral blood mononuclear cells can be detected in vivo using clinical MRI parameters in a therapeutic cell setting, *Sci. Rep.*, ***8***(1), 2018, 590
13.VOIGT, J.; CHRISTENSEN, J.; SHASTRI, V.P., Differential uptake of nanoparticles by endothelial cells through polyelectrolytes with affinity for caveolae, *Proceedings of the National Academy of Sciences*, ***111***(8), 2014, 2942-2947
14.VU-QUANG, H.; VINDING, M.S.; XIA, D.; NIELSEN, T.; ULLISCH, M.G.; DONG, M.; NIELSEN, N.C.; KJEMS, J., Chitosan-coated poly(lactic-co-glycolic acid) perfluorooctyl bromide nanoparticles for cell labeling in 19F magnetic resonance imaging, *Carbohydrate Polymers*, ***136***, 2016, 936-944
15.PISANI, E.; RINGARD, C.; NICOLAS, V.; RAPHAËL, E.; ROSILIO, V.; MOINE, L.; FATTAL, E.; TSAPIS, N., Tuning microcapsules surface morphology using blends of homo- and copolymers of PLGA and PLGA-PEG, *Soft Matter*, ***5***(16), 2009, 3054-3060
16.PISANI, E.; FATTAL, E.; PARIS, J.; RINGARD, C.; ROSILIO, V.; TSAPIS, N., Surfactant dependent morphology of polymeric capsules of perfluorooctyl bromide: influence of polymer adsorption at the dichloromethane-water interface, *Journal of colloid and interface science*, ***326***(1), 2008, 66-71
17.DIOU, O.; TSAPIS, N.; GIRAUDEAU, C.; VALETTE, J.; GUEUTIN, C.; BOURASSET, F.; ZANNA, S.; VAUTHIER, C.; FATTAL, E., Long-circulating perfluorooctyl bromide nanocapsules for tumor imaging by 19FMRI, *Biomaterials*, ***33***(22), 2012, 5593-5602

Manuscript received: 18.02.2020